

# Pulsar Wind Nebulae inside Supernova Remnants as Cosmic-Ray PeVatrons

Yutaka Ohira, Shota Kisaka, Ryo Yamazaki

Department of Physics and Mathematics, Aoyama Gakuin University, 5-10-1 Fuchinobe, Sagami-hara 252-5258, Japan

We propose that cosmic-ray PeVatrons are pulsar wind nebulae (PWNe) inside supernova remnants (SNRs). The PWN initially expands into the free expanding stellar ejecta. Then, the PWN catches up with the shocked region of the SNR, where particles can be slightly accelerated by the back and forth motion between the PWN and the SNR, and some particles diffuse into the PWN. Afterwards the PWN is compressed by the SNR, where the particles in the PWN are accelerated by the adiabatic compression. By using a Monte Carlo simulation, we show that particles accelerated by the SNR to 0.1 PeV can be reaccelerated to 1 PeV until the end of the PWN compression.

PACS numbers: 52.35.Tc; 52.65.Pp; 96.50.Pw; 96.50.S-; 97.60.Gb; 98.38.Mz

*Introduction.*— The origin of cosmic-ray (CR) PeVatrons is a long standing problem in the Astrophysics. The CR spectrum has a spectral break at  $\sim 10^{15}$  eV = 1 PeV (so called, the knee energy). The diffusive shock acceleration (DSA) at supernova remnants (SNRs) is believed to be the acceleration mechanism of CRs up to the knee energy [1]. Although recent gamma-ray observations support the idea [2], there are still many problems. One is the knee problem. It was estimated that SNRs cannot accelerate CRs to the knee energy for a parallel shock without a magnetic field amplification [3]. In order to accelerate CRs to the knee energy, magnetic fields must be amplified in the shock upstream region. Several mechanisms of the magnetic field amplification in the shock upstream region have been proposed [4]. However, no simulations demonstrate that the upstream magnetic field is sufficiently amplified to accelerate CRs to the knee energy. In contrast to the shock upstream region, magnetic fields are expected to be easily amplified to the equipartition level in the shock downstream region [5]. Super-Alfvénic turbulence amplifies the magnetic field by stretching the magnetic field line. The downstream turbulence is generated by interactions between upstream density fluctuations and the shock front. In addition, the downstream turbulence is generated by the Rayleigh-Taylor instability at the contact discontinuity. As a result, the magnetic field in the shocked region is amplified by the turbulence. If only the downstream magnetic field is amplified, the acceleration time scale of DSA is predominantly determined by the upstream residence time of accelerated particles, which depends on the shock velocity,  $u_{\text{sh}}$ , and the diffusion coefficient,  $D$ , [6]. Then the acceleration time scale is given by

$$t_{\text{acc}} \approx \frac{4D}{u_{\text{sh}}^2} = \frac{4cE}{3eu_{\text{sh}}^2 B_{\text{up}}} \approx 10^4 \text{ yr} \left( \frac{E}{1 \text{ PeV}} \right) \left( \frac{u_{\text{sh}}}{3 \times 10^3 \text{ km s}^{-1}} \right)^{-2} \left( \frac{B_{\text{up}}}{3 \mu\text{G}} \right)^{-1} \quad (1)$$

where we assume the shock compression ratio of 4, the Bohm diffusion coefficient,  $D = cE/3eB_{\text{up}}$ , and  $c, e, E$  and  $B_{\text{up}}$  are the speed of light, elementary charge, parti-

cle energy, and upstream magnetic field strength, respectively. After the free expansion phase ( $t > t_{\text{Sedov}}$ ), the velocity of the forward shock decreases with time. The Sedov time,  $t_{\text{Sedov}}$ , is given by

$$t_{\text{Sedov}} \approx 10^3 \text{ yr} \left( \frac{E_{\text{SN}}}{10^{51} \text{ erg}} \right)^{-\frac{1}{2}} \left( \frac{M_{\text{ej}}}{3 M_{\odot}} \right)^{\frac{5}{6}} \left( \frac{n}{0.1 \text{ cm}^{-3}} \right)^{-\frac{1}{3}}, \quad (2)$$

where  $E_{\text{SN}}, M_{\text{ej}}$  and  $n$  are the explosion energy, ejecta mass, and the ambient number density, respectively. From the condition,  $t_{\text{acc}} = t_{\text{Sedov}}$ , the maximum energy of particles accelerated at the forward shock is given by

$$E_{\text{max}} \approx 0.1 \text{ PeV} \left( \frac{E_{\text{SN}}}{10^{51} \text{ erg}} \right)^{\frac{1}{2}} \left( \frac{M_{\text{ej}}}{3 M_{\odot}} \right)^{-\frac{1}{6}} \left( \frac{n}{0.1 \text{ cm}^{-3}} \right)^{-\frac{1}{3}} \left( \frac{B_{\text{up}}}{3 \mu\text{G}} \right), \quad (3)$$

where  $u_{\text{sh}} = (2E_{\text{SN}}/M_{\text{ej}})^{1/2}$  is assumed. This is about 10 times smaller than the knee energy.

The other possible solution for the knee problem is DSA at the perpendicular shocks [7]. Since accelerated particles cannot propagate to the far upstream region, the acceleration time scale becomes small for the perpendicular shock. Although the injection to DSA was thought to be difficult for the perpendicular shock, it was showed by three-dimensional hybrid simulations that particles are injected to DSA at the perpendicular shock in a partially ionized plasma, so that particles are rapidly accelerated by the perpendicular shock [8]. However, DSA at the perpendicular shocks has another problem. For the case of the perpendicular shocks, the maximum energy is limited by the size of acceleration region,  $R$ . The available potential drop is  $\Delta\phi = RB_{\text{up}}u_{\text{sh}}/c$ , so that the maximum energy of accelerated protons is given by

$$E_{\text{max}} = e\Delta\phi \approx 0.1 \text{ PeV} \left( \frac{R}{10 \text{ pc}} \right) \left( \frac{B_{\text{up}}}{3 \mu\text{G}} \right) \left( \frac{u_{\text{sh}}}{3 \times 10^3 \text{ km s}^{-1}} \right) \quad (4)$$

which is again 10 times smaller than the knee energy. In order to accelerate CRs to the knee energy at the

perpendicular shock, we need an exceptional condition [9].

In this Letter, we propose a reacceleration mechanism from 0.1 PeV to 1 PeV by pulsar wind nebulae (PWNe) inside SNRs. As mentioned above, the magnetic field in the shocked region of SNRs is large enough to scatter high-energy particles. The magnetic field in young PWNe is also large compared with that in the interstellar medium, which is about  $B_{\text{PWN}} = 0.1 - 1$  mG [10]. The PWN initially expands into the freely expanding stellar ejecta toward the shocked region of the SNR. Since this system can be interpreted as two walls approaching each other, particles are accelerated, shuttling between the PWN and the shocked region of the SNR. After the PWN reaches the reverse shock of the SNR, the PWN is compressed and particles inside the PWN are accelerated by the adiabatic compression [11, 12]. In the next section, by using Monte Carlo simulation, we show that the PWN-SNR system actually accelerates particles from 0.1 PeV to 1 PeV.

*Monte Carlo simulations.*— In order to investigate the particle acceleration by the PWN-SNR system, we first provide evolution of an SNR and a PWN inside the SNR. As a first step, we consider a spherically symmetric structure. For constant ejecta and ambient density profiles, the approximate time evolution of the forward and reverse shock radii,  $R_{\text{SNR,fs}}$  and  $R_{\text{SNR,rs}}$ , are given by [13]. For a constant spindown luminosity of a pulsar and a constant ejecta density profile, the analytical solution for the time evolution of the PWN radius,  $R_{\text{PWN}}$ , is given by [12]. Fig 1 shows the time evolutions of the forward and reverse shock radii of the SNR and the radius of PWN, where we assume the constant ejecta profile with the ejecta mass of  $M_{\text{ej}} = 3 M_{\odot}$ , the explosion energy of  $E_{\text{SN}} = 10^{51}$  erg, the constant ambient matter profile with the density of  $n = 0.1 \text{ cm}^{-3}$ , and the constant pulsar spindown luminosity of  $L_{\text{sd}} = 3 \times 10^{38} \text{ erg s}^{-1}$ . For these parameters, the PWN catches up with the reverse shock of the SNR at  $t_c \approx 2 \times 10^3$  yr. Afterwards, the PWN is compressed by the shocked region of the SNR. In this Letter, we simply assume that the velocity of the PWN during the compression is  $v_{\text{PWN}} = -v_{\text{PWN}}(t_c)/2$  and the final size of the PWN is  $R_{\text{PWN}} = R_{\text{PWN}}(t_c)/5$ . Then, the PWN size becomes  $\approx 1.2$  pc at  $t_{\text{end}} \approx 5 \times 10^3$  yr. These assumptions are reasonable to simulate evolution of a spherical PWN [e.g. 14].

We next give the velocity structure in the PWN-SNR system. The expansion velocity of the shocked ejecta of the SNR in the observer frame is given by

$$v_{\text{SNR,shocked}} = \frac{R_{\text{SNR,rs}}/t - v_{\text{SNR,rs}}}{4} + v_{\text{SNR,rs}} \quad , \quad (5)$$

where we assume the compression ratio at the SNR reverse shock is 4, and  $v_{\text{SNR,rs}} = dR_{\text{SNR,rs}}/dt$  is the propagation velocity of the reverse shock in the observer frame. The expansion velocity of the PWN is given by

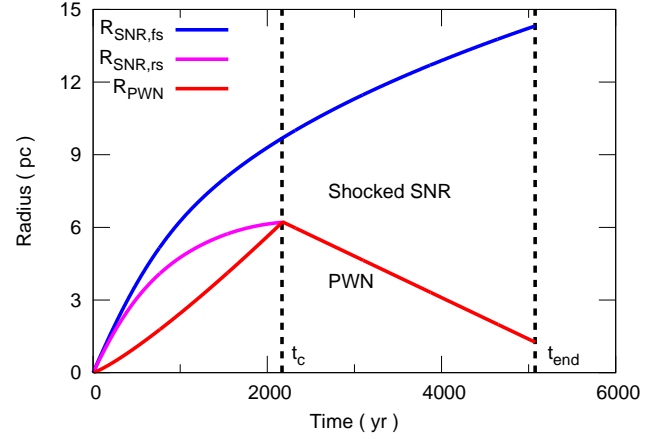


FIG. 1. Time evolution of the PWN radius (red) with a spindown luminosity of  $L_{\text{sd}} = 3 \times 10^{38} \text{ erg s}^{-1}$ , and radii of the forward (black) and the reverse shocks (blue) of the SNR with an explosion energy of  $E_{\text{SN}} = 10^{51}$  erg, an ejecta mass of  $M_{\text{ej}} = 3 M_{\odot}$ , and an ambient number density of  $n_{\text{ISM}} = 0.1 \text{ cm}^{-3}$ .

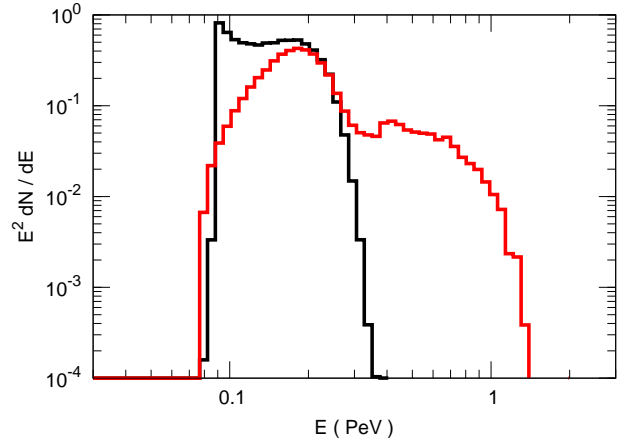


FIG. 2. Energy spectrum of reaccelerated particle at the end of the PWN compression,  $t = t_{\text{end}}$ . The black and red histograms are for particles that were in the SNR and the PWN regions at time when the PWN reached the reverse shock of the SNR,  $t = t_c$ . The initial energy is 0.1 PeV.

$v_{\text{PWN}} = dR_{\text{PWN}}/dt$  [12]. Until the PWN reaches the reverse shock of the SNR, the velocity structures in both the SNR and the PWN are assumed to be uniform in this Letter. After the PWN interacts with the reverse shock of the SNR, the velocity structure in the PWN is assumed as

$$\vec{v}_{\text{PWN,in}}(t, \vec{r}) = -\frac{v_{\text{PWN}}(t_c)}{2} \frac{\vec{r}}{R_{\text{PWN}}(t)} \quad . \quad (6)$$

Since the shocked region of the SNR and the PWN region are expected to be highly turbulent [15], motion of high-energy particles could be approximated as the random walk. Using the above hydrodynamical structure, we perform a test-particle Monte Carlo simula-

tion. Simulation particles are isotropically scattered in the local fluid frame. The scattering time is assumed to be the Bohm scattering,  $t_{\text{sc}} = \Omega_c^{-1}(E/m_p c^2)$ , where  $\Omega_c \approx 10^{-2} \text{ s}^{-1}(B/1 \text{ } \mu\text{G})$  is the proton cyclotron frequency,  $E$  is the particle energy, and  $m_p$  is the proton mass. During the compression phase of the PWN ( $t_c < t < t_{\text{end}}$ ), we do not follow the particle motion once the particle escapes from the PWN.

In this Letter, we set the magnetic field to be  $B = 3 \times 10^2 \text{ } \mu\text{G}$  both in the PWN and the shocked region of the SNR, and  $B = 0$  in the free expanding ejecta. So that, particles are not scattered in the free expanding ejecta. At  $t = 10^3 \text{ yr}$ , we impulsively inject simulation particles isotropically on the reverse shock sphere,  $r = R_{\text{SNR,rs}}$ . Since the SNR can accelerate particles to about 0.1 PeV (see introduction), we set the initial energy to be 0.1 PeV.

Fig 2 shows the energy spectrum of the accelerated particles at the end of the PWN compression ( $t = t_{\text{end}}$ ). The black histogram shows the energy spectrum of particles that were in the shocked region of the SNR when the PWN reached the reverse shock of the SNR ( $t = t_c$ ). They are accelerated up to twice the initial energy by the back and forth motion between the PWN and the shocked region of the SNR. However, they are not accelerated by the PWN compression. The energy gain in each cycle is  $\Delta E/E \sim \Delta v/c$ , where  $\Delta v = v_{\text{SNR,shocked}} - v_{\text{PWN}}$  is the relative velocity. The time scale in each cycle is  $\Delta t \sim \Delta R/c$ , where  $\Delta R = R_{\text{SNR,rs}} - R_{\text{PWN}}$  is the relative distance. Then, the acceleration time scale for the reciprocation is given by  $t_{\text{acc}} = \Delta t(E/\Delta E) \sim \Delta R/\Delta v$  that is the same as the dynamical time scale in which the PWN catches up with the SNR reverse shock. Since the acceleration time scale,  $t_{\text{acc}}$ , does not depend on the particle energy, it takes  $t_{\text{acc}}$  to accelerate particles to twice the initial energy. Therefore, the maximum energy during the approaching phase becomes twice the initial energy.

The red histogram shows the energy spectrum of particles confined in the PWN at  $t = t_c$ . They are further accelerated to 1 PeV by the PWN compression. The maximum energy gain during the compression is  $\Delta E/E \sim R_{\text{PWN}}(t_{\text{end}})/R_{\text{PWN}}(t_c) = 5$ , so that the particles are finally accelerated to ten times the initial energy. Hence, the PWN-SNR system can accelerate particles to the knee energy.

*Discussion.*— We first discuss on the acceleration of heavy nuclei. CRs are organized not only by protons but also by heavy nuclei whose origin is also a long standing problem [16]. Since the supernova ejecta is metal rich, the reverse shock propagating into the supernova ejecta is thought to be the origin of heavy CR nuclei [17]. However, the maximum energy of the accelerated particle at the reverse shock is not so large because the magnetic field in the expanding supernova ejecta is expected to be very small. Furthermore, particles accelerated by the reverse shock suffer the adiabatic cooling. Our reacceleration model can boost the maximum energy of acceler-

ated heavy nuclei, so that the PWN-SNR system could be important for the production of heavy CR nuclei.

Next, we discuss the energy spectrum of accelerated particles. As shown in Fig 2, most particles are boosted by only twice and a few particles are accelerated to 1 PeV. Therefore, the spectrum seems to be too steep to explain the CR spectrum observed at the Earth. We considered only particle diffusion by the magnetic field fluctuation, but diffusion by turbulence could be significant. If more particles diffuse deeper inside the PWN by the turbulent diffusion, more particles will be accelerated to 1 PeV. Furthermore, since there is the potential difference of about 1 PV in the PWN, protons could be accelerated to 1 PeV by drifting the toroidal magnetic field [18], which was not considered in this Letter. Hence, further studies are needed to understand the energy spectrum of particles accelerated by the PWN-SNR system. In addition, to understand the source spectrum of CRs that are injected to our Galaxy, we have to consider the particle spectrum that have escaped from the SNR [19]. Therefore, when and how accelerated particles escape from the PWN-SNR system is an important issue. This issue could be addressed by gamma-ray observations of the PWN-SNR system like SNR G327.1-1.1, W44 and so on.

As a first step, in this Letter we assumed spherical symmetry for the PWN-SNR system and the Bohm scattering with constant magnetic field strength for the random walk. In reality, a pulsar has a kick velocity, and the supernova ejecta, the ambient matter, the PWN have asymmetry. In addition, the Rayleigh-Taylor instability amplifies the asymmetry [20], so that the PWN-SNR system is actually more complicated. In particular, the strong turbulence could play an important role, that amplifies the magnetic field, affecting the particle motion [21], and accelerates particles by turbulent acceleration [22]. In order to address above problems, we need a more realistic magnetohydrodynamical simulation. This will be addressed in future work.

*Summary.*— We have proposed that PWNe inside SNRs are the CR PeVatron. Firstly, the SNR shock accelerates protons to  $\sim 0.1 \text{ PeV}$ . Then, the protons diffuse into the interior of the SNR and are reaccelerated to  $\sim 0.2 \text{ PeV}$  by the back and forth motion between the SNR and the PWN. Finally, the protons diffuse into the PWN and are accelerated to  $\sim 1 \text{ PeV}$  by the adiabatic compression while the PWN is compressed by the SNR. In addition, we have argued that the PWN-SNR system could be the origin of heavy CR nuclei.

Numerical computations were carried out on the XC30 system at the Center for Computational Astrophysics (CfCA) of the National Astronomical Observatory of Japan. This work was supported in part by Grants-in-Aid for Scientific Research of the Japanese Ministry of Education, Culture, Sports, Science and Technology No.16K17702(YO), No.16J06773(SK), and No.15K05088(RY).

- 
- [1] W. I. Axford, E. Leer, and G. Skadron, Proc. 15th Int. Cosmic Ray Conf., (Plovdiv: Bulgarian Academy of Sciences), **11**, 132 (1977); G. F. Krymsky, Dokl. Akad. Nauk SSSR **234**, 1306 (1977); A. R. Bell, Mon. Not. R. Astron. Soc. **182**, 147 (1978); R. D. Blandford and J. P. Ostriker, Astrophys. J. **221**, L29 (1978)
- [2] Y. Ohira, K. Murase, and R. Yamazaki, Mon. Not. R. Astron. Soc. **182**, 147 (2011); M. Ackermann, et al. Science, **339**, 807 (2013)
- [3] P. O. Lagage, and C. J. Cesarsky, Astron. Astrophys. **125**, 249 (1983)
- [4] A. R. Bell, Mon. Not. R. Astron. Soc. **353**, 550 (2004); M. A. Malkov, P. H. Diamond, and R. Z. Sagdeev, PPCF, **52**, 124006 (2010); Y. Ohira, and F. Takahara, Astrophys. J. **721**, L43 (2010); Y. Ohira, Astrophys. J. **758**, 979 (2012)
- [5] J. Giacalone and J. R. Jokipii, Astrophys. J. **663**, L41 (2007); T. Inoue, R. Yamazaki, and S. Inutsuka, Astrophys. J. **695**, 825 (2009); F. Guo, S. Li, H. Li, J. Giacalone, J. R. Jokipii, and D. Li, Astrophys. J. **747**, 98 (2012); D. Caprioli and A. Spitkovsky, Astrophys. J. **765**, L20 (2013); Y. Ohira, Astrophys. J. **817**, 137 (2016)
- [6] Y. Ohira, and R. Yamazaki, arXiv:1609.02266 (2016); L. O'C. Drury, Rep. Prog. Phys. **46**, 973 (1983)
- [7] J. R. Jokipii, Astrophys. J. **313**, 842 (1987)
- [8] Y. Ohira, Astrophys. J. **827**, 36 (2016)
- [9] M. Takamoto, and J. G. Kirk, Astrophys. J. **809**, 29 (2015)
- [10] S. J. Tanaka, and F. Takahara, Astrophys. J. **715**, 1248 (2010); D. F. Torres, A. Cillis, J. Martin, and E. de Ona Wilhelmi, JHEAp, **1**, 31 (2014)
- [11] J. M. Blondin, R. A. Chevalier, and D. M. Frierson, Astrophys. J. **563**, 806 (2001)
- [12] E. van der Swaluw, A. Achterberg, Y. A. Gallant, and G. Tóth, Astron. Astrophys. **380**, 309 (2001)
- [13] C. F. McKee, and J. K. Truelove, Phys. Rep. **256**, 157 (1995)
- [14] J. D. Gelfand, P. O. Slane, and W. Zhang, Astrophys. J. **703**, 2051 (2009)
- [15] O. Porth, S. S. Komissarov, and R. Keppens, Mon. Not. R. Astron. Soc. **438**, 278 (2014)
- [16] Y. Ohira, N. Kawanaka, and K. Ioka, PRD **93**, 083001 (2016)
- [17] V. Ptuskin, V. Zirakashvili, and E. S. Seo, Astrophys. J. **763**, 47 (2013)
- [18] A. R. Bell, Mon. Not. R. Astron. Soc. **257**, 493 (1992); A. R. Bell, and S. G. Lucek, Mon. Not. R. Astron. Soc. **283**, 1083 (1996)
- [19] Y. Ohira, K. Murase, and R. Yamazaki, Astron. Astrophys. **513**, A17 (2010); Y. Ohira, and K. Ioka, Astrophys. J. **729**, L13 (2011)
- [20] E. van der Swaluw, T. P. Downes, and R. Keegan, Astron. Astrophys. **420**, 937 (2004)
- [21] O. Porth, M. J. Vorster, M. Lyutikov, and N. E. Engelbrecht, Mon. Not. R. Astron. Soc. **460**, 4135 (2016)
- [22] Y. Ohira, Astrophys. J. **767**, L16 (2013)